

Contents lists available at ScienceDirect

# Journal of the Mechanical Behavior of Biomedical Materials

journal homepage: www.elsevier.com/locate/jmbbm



#### Technical note

# A specialized protocol for mechanical testing of isolated networks of type II collagen

Phoebe Szarek <sup>a</sup>, David M. Pierce <sup>a,b,\*</sup>

- a Department of Biomedical Engineering, University of Connecticut, Storrs, CT, United States of America
- <sup>b</sup> Department of Mechanical Engineering, University of Connecticut, Storrs, CT, United States of America

## ARTICLE INFO

#### Keywords: Collagen fibers Collagen networks Type II collagen Cartilage

## ABSTRACT

The mechanical responses of most soft biological tissues rely heavily on networks of collagen fibers, thus quantifying the mechanics of both individual collagen fibers and networks of these fibers advances understanding of biological tissues in health and disease. The mechanics of type I collagen are well-studied and quantified. Yet no data exist on the tensile mechanical responses of individual type II collagen fibers nor of isolated networks comprised of type II collagen. We aimed to establish methods to facilitate studies of networked and individual type II collagen fibers within the native networked structure, specifically to establish best practices for isolating and mechanically testing type II collagen networks in tension. We systematically investigated mechanical tests of networks of type II collagen undergoing uniaxial extension, and quantified ranges for each of the important variables to help ensure that the experiment itself does not affect the measured mechanical parameters. Specifically we determined both the specimen (establishing networks of isolated collagen, the footprint and thickness of the specimen) and the mechanical test (both the device and the strain rate) to establish a repeatable and practical protocol. Mechanical testing of isolated networks of type II collagen fibers leveraging this protocol will lead to better understanding of the mechanics both of these networks and of the individual fibers. Such understanding may aid in developing and testing therapeutics, understanding interconstituent interactions (and their roles in bulk-tissue biomechanics), investigating mechanical/biochemical modifications to networked type II collagen, and proposing, calibrating, and validating constitutive models for finite element analyses.

# 1. Introduction

The mechanical responses of most soft biological tissues rely heavily on networks of protein fibers including collagen (Broom and Marra, 1986; Zhu et al., 1993; Aspden, 1994; Hukins et al., 1999). Collagen fibers contribute to the mechanical response and stiffness of such tissues, particularly in tension, often with tensile stiffnesses orders of magnitude above the contributions of other constituents (Ottani et al., 2001; McNulty et al., 2006; Taye et al., 2019; Wang et al., 2018). Many diseases of soft tissues alter the microstructure of collagen fibers or networks of collagen via biochemical (Onur et al., 2014; Wan et al., 2021) or mechanical (Andriacchi and Mündermann, 2006; Cai et al., 2017) means. Study of the mechanics of both individual collagen fibers and networks of these fibers advances understanding of biological tissues in health and disease.

Researchers have identified 28 types of human collagen (to date) and categorized these based on amino-acid composition (Ricard-Blum, 2011). Type I collagen is the most prevalent type in the human body

and is found in, e.g. skin, tendon, bones, and arteries. The mechanics of type I collagen are well-studied and quantified. To characterize individual type I fibers researchers employ tensile or bending tests on isolated type I collagen fibers ( $\varnothing\sim350$  nm–1  $\mu m$ ) using a variety of methods including atomic force microscopy, microtensile testing, and specialized microelectromechanical systems (Miyazaki and Hayashi, 1999; Eppell et al., 2006; van der Rijt et al., 2006; Wenger et al., 2007; Gestos et al., 2013; Liu et al., 2016; Quigley et al., 2018).

The next most prevalent collagen in the human body is type II, which plays a significant mechanical role in many tissues, e.g. articular cartilage, vitreous humor (within the eye), and fibrocartilage within intervertebral discs. Yet no data exist on the tensile mechanical responses of individual type II collagen fibers nor of networks comprised of type II collagen. Characterizing the unique properties of type II collagen will advance understanding of the mechanics of human and engineered tissues.

<sup>\*</sup> Correspondence to: Department of Mechanical Engineering, University of Connecticut, 191 Auditorium Road, Storrs, CT 06269, United States E-mail address: dmpierce@engr.uconn.edu (D.M. Pierce).

Two difficulties complicate the mechanical study of type II collagen: (1) the size of the fibers and (2) the difficulty in isolating fibers. Individual type II collagen fibers have a diameter ~ 20–200 nm (Gottardi et al., 2016; Szarek et al., 2020), much smaller than type I, but larger than DNA ( $\varnothing \sim 2$  nm) and membrane macromolecules (of similar diameter). Thus methods used to quantify the mechanics of type I collagen do not translate well to type II. Similarly, individual type II collagen fibers may be too large for methods applied to smaller molecules such as optical and magnetic tweezers for DNA (Bustamante et al., 2003; Goss and Croquette, 2002). Additionally, obtaining in-vivo-like type II collagen fibers proves difficult. Complications arise in isolating type II collagen from tissues without disassembling it to a subfibrillar level, and in growing type II fibers from collagen molecules (Kadler et al., 2008; Karvonen et al., 1991; Kuijer et al., 1985; Lee and Piez, 1983). In both cases the resulting fibers do not reflect the structure of native collagen fibers within tissues such as cartilage.

Although tensile tests on thin sheets of cartilage have aided our understanding of bulk-tissue mechanics (Kempson et al., 1973; Elliot et al., 1999; Huang et al., 2005; Sasazaki et al., 2006), the macromechanics of cartilage derive from complex micromechanical interactions of proteoglycans (5%–10% wet weight), collagens, and electrolytic fluid, e.g. osmotic swelling driven by the fixed-charge density of proteoglycans pretensions the network of collagen even in the absence of external loading (Kempson et al., 1970; Wang et al., 2018). Such interactions occur in tissue-level experiments and complicate direct study of the mechanics of collagen networks and of individual collagen fibers.

We aimed to establish methods to study networked and individual type II collagen fibers within a native networked structure, specifically to establish best practices for isolating and mechanically testing type II collagen networks in tension. These methods include: (1) establishing the specimens (i.e. footprint and thickness of isolated network of collagen) and (2) establishing a repeatable tensile test (i.e. testing device, strain rate). Finally, we consider minimizing time and cost while maximizing repeatability to establish an efficient and practical research method.

#### 2. Materials and methods

## 2.1. Establishing the specimen

We obtained healthy specimens from bovine knees harvested from animals less than 36 months of age. If not immediately used to prepare specimens, we stored knees at  $-20^{\circ}$ C either with the joint capsule intact or in phosphate-buffered saline (PBS) and for a maximum of one freezethaw cycle (Szarko et al., 2010). We extracted full-thickness ~ 10 mm by ~ 20 mm cuboid specimens from the patellofemoral groove for all subsequent analyses. Within the patellofemoral groove we oriented the specimens with the long axis parallel to the estimated split-line direction (SLD) (Williamson et al., 2003) and then we determined the true local SLD by pricking the articular surface (outside the area intended for the final test specimen) with a dissecting needle dipped in India ink (Below et al., 2002). To focus on the superficial zone we microtomed 200  $\mu m$  thick slices of cartilage using a rotary microtome (HM 355 S, Microm International, Walldorf, DE) (Mow et al., 2005). From the pieces of the superficial zone of the patella we prepared specimens for testing the enzymatic digestion. From the strips of the superficial zone from the patellofemoral groove we prepared specimens for refining the dimensions of the tensile specimen, and establishing parameters of the mechanical test.

#### 2.1.1. Networks of isolated collagen

We used a 5 mm diameter circular punch to create uniform specimens of the superficial zone and establish our enzymatic digestion protocols based on trypsin (Chun et al., 1986; Torzilli et al., 1997). We tested 0.0, 0.125, 0.25, 1.0, and 2.0 mg/mL concentrations of trypsin (from porcine pancreas, Sigma Aldrich, St. Louis, MO) in a buffer of 0.05 M sodium phosphate and 0.15 M sodium chloride for durations of 18, 24, 36, and 48 h at 37°C. We tested n = 6 specimens in each combination of concentration and duration. After digestion we rinsed specimens three times for five minutes (each time) in buffer using a rocker table (Bellco Biotechnology, Vineland, NJ) at room temperature. Next we quantified the amount of PG remaining in each specimen using a glycosaminoglycan assay (Chondrex, Inc., Redmond, WA) after papain solubilization (Chondrex). We compared the resulting quantities against a set of negative controls determined using the amount of PG within the tissue and in the solution of the enzyme-free trials. After establishing which protocols sufficiently digested PG we repeated those digestions using new specimens and assessed the collagen content within the specimens under the same digestion protocols. After rinsing the tissue with the buffer as before, we quantified the amount of collagen in the specimens using a Sirius Red-based assay (Chondrex) after pepsin solubilization (Chondrex). We compared the collagen content in the specimens to one another and to untreated controls (Maier et al., 2019a,b). Finally, we carefully remeasured the dimensions of the specimen after digestion.

#### 2.1.2. Footprint of the specimen

We utilized finite element analyses to understand the effects of specimen geometry on the homogeneity of stresses within the gauge region of our proposed dumbbell-shaped specimens of type II collagen (PG-depleted cartilage) under tensile loading. We meshed a parametric, quarter-symmetry model of the specimen with eight-node hexahedral elements, and ensured relatively high mesh densities at and around the gauge region of the dumbbell shape. Specifically, we included at least three elements in the through-thickness direction to ensure that these were not overly stiff in bending. We then used h-refinement within the footprint (plane parallel to the articular surface) to ensure that the stress/strain results of interest changed by less than one percent upon subsequent mesh refinements. We employed our image-driven constitutive model of cartilage but we decreased the stiffness (shear modulus) of the isotropic matrix to five percent of the baseline value and we correspondingly increased the permeability to model networked type II collagen (PG-depleted cartilage) within a continuum framework (Wang et al., 2018; Pierce et al., 2016). We simulated the tensile test by applying an axial displacement equal to the gauge length (quasistatically) to the edge clamped during the test. We evaluated the feasibility and suitability of each specimen design by assessing the maximum displacement and force (in light of the displacement range and load capacity of the microtensile device), and by quantifying the heterogeneity in the first principal stresses within the gauge region by calculating the percent difference between the principal stresses predicted at the center of the gauge region to those at the corresponding lateral edge (see red dots within Fig. 1).

We based the initial dimension of our specimen on the microtensile testing guidelines from ASTM D1708-13 (American Society for Testing Materials, 2013). We fixed the clamping width and length to 9 mm and 4.3 mm, respectively, and the thickness to 200  $\mu \rm m$ . We then parametrically varied dimensions that may affect the failure stress and distribution of stresses, see Fig. 1. Specifically, we varied the following dimensions at 0.5 mm increments as specified (all given in mm): gauge length  $l_g \in [3.0, 8.0]$ , radius  $r \in [1.0, 4.0]$ , gauge width  $w_g \in [1.0, 7.0]$ , and total length  $l_t \in [13.6, 24.6]$ . Fixing the both clamping length and width (i.e. total width) created an interdependence between gauge width and radius.

We performed all simulations in FEBio (version 2.5, University of Utah, Salt Lake City, UT Maas et al., 2012).

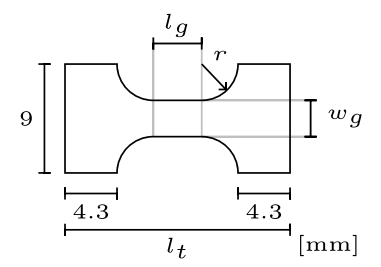


Fig. 1. Specimen dimensions. We fixed the clamping width and length to 9 mm and 4.3 mm, respectively, and parametrically varied the gauge width  $w_{\rm g}$ , gauge length  $l_{\rm g}$ , and radius r at 0.5 mm increments. The total length  $l_{\rm f}$  depends on the gauge length, radius, and the fixed clamping length. We evaluated heterogeneity within the gauge region by calculating the percent difference between the principal stresses calculated at the center of the gauge region to those at the corresponding lateral edge (red dots). Dimensions in mm.

#### 2.1.3. Thickness of the specimen

We compared the mechanical responses (detailed in §2.3) measured using specimens with thicknesses  $T \in [100, 200]~\mu m$  in 20  $\mu m$  increments, i.e. 100, 120, 140, 160, 180, and 200  $\mu m$ . We used a custom dumbbell-shaped cutter to produce uniform specimens from the thin sheets of cartilage, completed the digestion of PG, and performed tensile testing at a displacement rate of 300  $\mu m$  per second. We compared the measured mechanical responses as a function of thickness using statistical analyses (detailed in §2.4) to establish an optimal range of thicknesses for subsequent specimens.

#### 2.2. Establishing the mechanical test

## 2.2.1. Device

We performed all tensile tests using our custom-built microtensile device with a displacement range of 12.5 mm (resolution: 2.5  $\mu$ m; 21H4AC-2.5-907, Ametek, Haydon Kerk, Waterbury, CT) and a force capacity of 20 N (resolution: 0.3 mN; JRS1-10 N, Forsentek, Shenzhen, CN) (Huang et al., 2005; Kempson et al., 1973; Sasazaki et al., 2006). We kept tissues hydrated in PBS at 25°C and aligned specimens with the principal fiber orientation (determined using the SLD method). To improve the contact area for clamping we gripped specimens using cyanoacrylate glue (Loctite, Henkel AG & Co., Düsseldorf, DE) and sandpaper (200 grit). We then mounted the fluid-saturated specimens in the device and allowed them to equilibrate for 300 s. Finally, we controlled the displacement putting the specimens in tension at the specified displacement (strain) rate (§2.2.2) until rupture, and monitored testing to ensure failure occurred within the gauge region. We recorded both displacement and force at a sampling frequency of 10 Hz.

#### 2.2.2. Strain rate

Once we finalized the dimensions of the dumbbell-shaped specimens we probed the effects of strain rate on the resulting mechanical data. We used our custom dumbbell-shaped cutter to produce uniform specimens from the thin sheets of cartilage ( $T=200~\mu m$ ), completed the digestion of PG, and performed tensile testing at a range of displacement rates. We compared the mechanical responses (detailed in §2.3) measured using tests with displacement rates of 150, 300, 450, 600, 750, 900, 1050, 1200, 1500, 1800, 2400, 3000, 3600, 4200, 4500, and 6000  $\mu m$  (equivalent to strain rates of 1.5, 3, 4.5, 6, 7.5, 9, 10.5, 12, 15, 18, 24, 30, 36, 42, 45, 60%/min). We compared the measured mechanical responses as a function of displacement rate (to probe rate dependence) using statistical analyses (detailed in §2.4) to establish an optimal range of displacement rates for subsequent tensile tests.

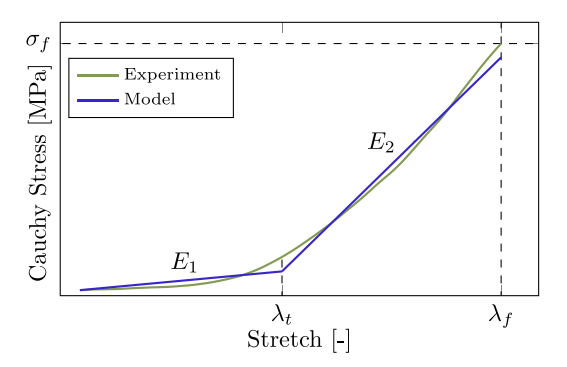


**Fig. 2.** Bilinear fit of experimental data. Representative data and fit: we fit our experimental data (Cauchy stress versus stretch) generated from tensile tests of networks of type II collagen (green) to the bilinear model (1), (blue) using three parameters: initial modulus  $E_1$ , transition stretch  $\lambda_t$ , and final modulus  $E_2$ . We also extracted the failure stress and failure stretch,  $\sigma_f$  and  $\lambda_f$  respectively.

#### 2.3. Mechanical analyses

Using the custom device we applied displacement at a specified rate and we measured axial force, resulting in force F and displacement d data as a function of time t. We calculated Cauchy stress  $\sigma$  from our measured force data using  $\sigma(t) = F(t)\lambda(t)/A$ , where A is the reference cross-sectional area and  $\lambda(t) = l(t)/l_0$  is the stretch ratio calculated by normalizing the current grip-to-grip length  $l(t) = l_0 + d(t)$  normalized by the initial grip-to-grip length  $l_0$  (note that strain  $\varepsilon(t) = \lambda(t) - 1$ ) (Stender et al., 2018; Wale et al., 2021). We ensured, both experimentally and computationally, that the grip-to-grip stretch approximated the true stretch within the gauge region (see Fig. 5, Appendix A). In our computational, cf. modeling in §2.1.2, and experimental analyses the difference between these stretches was less than 1.0% and  $3.8 \pm 2.2\%$ , respectively.

We assumed incompressibility and used the calculated Cauchy stresses versus stretches for all subsequent analyses (Park et al., 2004; Stender et al., 2018). We smoothed the stress-stretch data by first decreasing our sampling rate by a factor of five (i.e. to 2 Hz) then applying a smoothing filter using the LOESS method with a span of 10%. We defined the failure stress  $\sigma_f$  as the maximum Cauchy stress achieved during the test, and the failure stretch  $\lambda_f$  as the corresponding stretch. We fit the resulting mechanical responses ( $\sigma$  vs.  $\lambda$ ) of the collagen networks to five different mathematical models: linear (one parameter), exponential (two), bilinear (three), exponential-linear (four), and linear-exponential (four). Preliminary tests found that the bilinear model (using three parameters: initial modulus  $E_1$ , transition stretch  $\lambda_t$ , and final modulus  $E_2$ ) outperformed the other four models in fitting the bulk experimental data as evaluated by the adjusted Rsquared values (data not shown, R-squared > 0.98 for bilinear fits in preliminary tests). Thus, for all subsequent analyses we selected the bilinear model (1) as shown in Fig. 2. We also calculated the percent transition as  $100(\lambda_t/\lambda_f)$  in order to create a normalized transition measure independent of the failure stretch.

$$\sigma = \begin{cases} E_1(\lambda - 1) & \text{if } \lambda < \lambda_t, \\ E_2(\lambda - \lambda_t) + E_1(\lambda_t - 1) & \text{if } \lambda \ge \lambda_t. \end{cases}$$
 (1)

We completed all analyses using MATLAB R2019a (The MathWorks, Inc., Natick, MA).

## 2.4. Statistical analyses

To establish the digestion protocol, we used a two-variable regression with duration of digestion and trypsin concentration as variables. To establish the range of appropriate specimen thicknesses, we used a two-variable regression with thickness and donor knee as variables to

**Table 1**Mass percent proteoglycan remaining post digestion (% Mean Standard Deviation, n = 6 for each group) where we did not test the combinations with –. We propose the digestion protocol using 0.5 mg/mL trypsin for 18 h to reliably reduce the proteoglycan content to less than five percent of the original while preserving collagen network (See Fig. 6, Appendix B).

DigestionL duration (h)	Trypsin concentration (mg/mL)					
	0.0	0.125	0.25	0.5	1.0	2.0
18	82.5 ± 7.21	4.58 ± 1.86	$2.65 \pm 1.63$	2.06 ± 1.67	$2.39 \pm 1.20$	_
24	$87.4 \pm 4.79$	_	$2.27 \pm 0.37$	$1.39 \pm 0.86$	$1.15 \pm 1.31$	$1.61 \pm 0.50$
36	$88.3 \pm 7.76$	$4.15 \pm 2.17$	$3.50 \pm 1.10$	$2.28 \pm 0.89$	$0.52 \pm 0.10$	_
48	$84.2 \pm 4.85$	-	$1.25\pm0.81$	$1.34 \pm 0.65$	$1.54 \pm 0.39$	$1.13 \pm 0.39$

assess effects on measured mechanical parameters (i.e. parameters of the bilinear model, failure stress, failure stretch, percent transition, cf. §2.2). Similarly, to establish the range of appropriate strain rates, we used two-variable regression with displacement rate and donor knee as variables to assess effects on measured mechanical parameters. To probe differences between groups by thickness and differences between groups by rate, we used Student's *t*-tests and *F*-tests to compare means and variances, respectively. We used p < 0.05 for statistical significance and completed all analyses using Excel 2016 (Microsoft Corporation, Redmond, WA).

#### 3. Results

#### 3.1. Networks of isolated collagen

In Table 1 we show the percent PG remaining after each enzymatic digestion protocol we tested. We found no significant differences in the collagen content between any of the enzymatic digestion protocols and the untreated, healthy controls (see Fig. 6, Appendix B). We propose the digestion protocol using 0.5 mg/mL trypsin for 18 h. This protocol reliably reduces PG content to less than 5% of the original in a relative short period of time while preserving the network of collagen (see Fig. 6, Appendix B). The dimensions of the specimens did not change significantly before and after digestion (data not shown). The 2-D deformation gradient mapping the motion from the pre- to post-digestion configurations was equal to the identity (and the Jacobian equal to unity).

## 3.2. Footprint of the specimens

We completed parametric analyses on all combinations of the dimensions, i.e. gauge length ( $l_g \in [3.0, 8.0]$ ), radius ( $r \in [1.0, 4.0]$ ), gauge width ( $w_g \in [1.0, 7.0]$ ), and total length ( $l_t \in [13.6, 24.6]$ ) resulting in 36 unique simulations (§2.1.2). In these simulations the heterogeneity in the first principal stresses (i.e. the difference of first principal stress at the center of the gauge region of the specimen compared to the corresponding edge) varied from 0.0% to 16.4%. The total length of the specimens ranged from 13 to 27 mm and based on the displacement range of the microtensile device, the maximum possible strain varied from 78% to 179%. The principal stresses at the center node varied from 2.4 to 11.8 MPa generating an axial force of 0.56 to 11.8 N.

We propose the final dimensions of the dumbbell-shaped specimen as follows: gauge length  $l_{\rm g}=4$  mm, radius r=3 mm, gauge width  $w_{\rm g}=3$  mm, and total length  $l_{\rm f}=18.6$  mm. These dimensions create a relatively small specimen with a nearly homogeneous distribution of first principal stresses within the gauge region under uniaxial extension, and generated failure stresses and failure stretches in a range suitable for the testing device. The difference in first principal stress at the center point versus the corresponding edge was 1.9% (see Fig. 8, Appendix C).

#### 3.3. Thickness of the specimens

We compared the mechanical parameters ( $\sigma_f$ ,  $\lambda_f$ ,  $E_1$ ,  $\lambda_t$ ,  $E_2$ , and percent transition) generated using specimens with thicknesses of 100, 120, 140, 160, 180, and 200  $\mu$ m, see Fig. 3 and Appendix D.

We found no significant effect of donor knee on any of the measured mechanical parameters. The failure stress  $\sigma_f$  determined from 100  $\mu m$ thick specimens was significantly different than all other groups (p < 10.04 for all comparisons, Fig. 3a). We also found similar significance for the final modulus  $E_2$  determined from 100 µm thick specimens (p < 0.03for all comparisons). For both of these parameters, we found no other significant differences between thickness groups. The transition stretch of the 180  $\mu m$  specimens was significantly different from that of the 120, 140, and 160  $\mu$ m specimens (p = 0.027, 0.008, 0.021, respectively, Fig. 3b). The failure stretch  $\lambda_f$  determined from 180 µm thick specimens was also significantly different from the failure stretches determined from all groups of thinner specimens. The transition stretch  $\lambda_t$  determined from 100 µm and 180 µm thick specimens was approaching significance (p = 0.068). Finally, when comparing the coefficients of variance of all mechanical parameters, we found no significant difference between the variance of any parameters determined using specimens with 140 μm and 160 μm thicknesses (Fig. 3c).

We propose that specimens should be prepared with a thickness in the range 140–160  $\mu m$  to ensure mechanical results are independent of thickness.

#### 3.4. Device

We successfully designed, built, calibrated, and employed our device using readily-available components.

#### 3.5. Strain rate

We compared the mechanical parameters ( $\sigma_f$ ,  $\lambda_f$ ,  $E_1$ ,  $\lambda_t$ ,  $E_2$ , and percent transition) generated using strain rates ranging from (displacement rates ranging from 150 to 6000  $\mu$ m), see Fig. 4.

In the range tested we found no significant effects of displacement rate on any of the resulting mechanical parameters.

We propose that a displacement rate in the range 150 to  $6000~\mu m/min$  (1.5–60%/min) to ensure mechanical results are independent of displacement/strain rate.

## 4. Discussion

In light of the mechanical importance of type II collagen (both networked and individual fibers) we established a repeatable and practical protocol for testing networks of isolated type II collagen. We systematically investigated test variables that may affect the measured mechanical responses of these networks undergoing uniaxial extension, and established ranges for each of the important variables (e.g. thickness of the specimens, strain rate of testing) to help ensure that the experiment itself does not affect the measured mechanical parameters. Throughout this effort we also sought practicality, proposing a reasonable best practice while minimizing cost and time. To facilitate application of our protocol we provide a step-by-step guide for isolating and tensile testing of networks of type II collagen sourced from bovine articular cartilage in Appendix E.

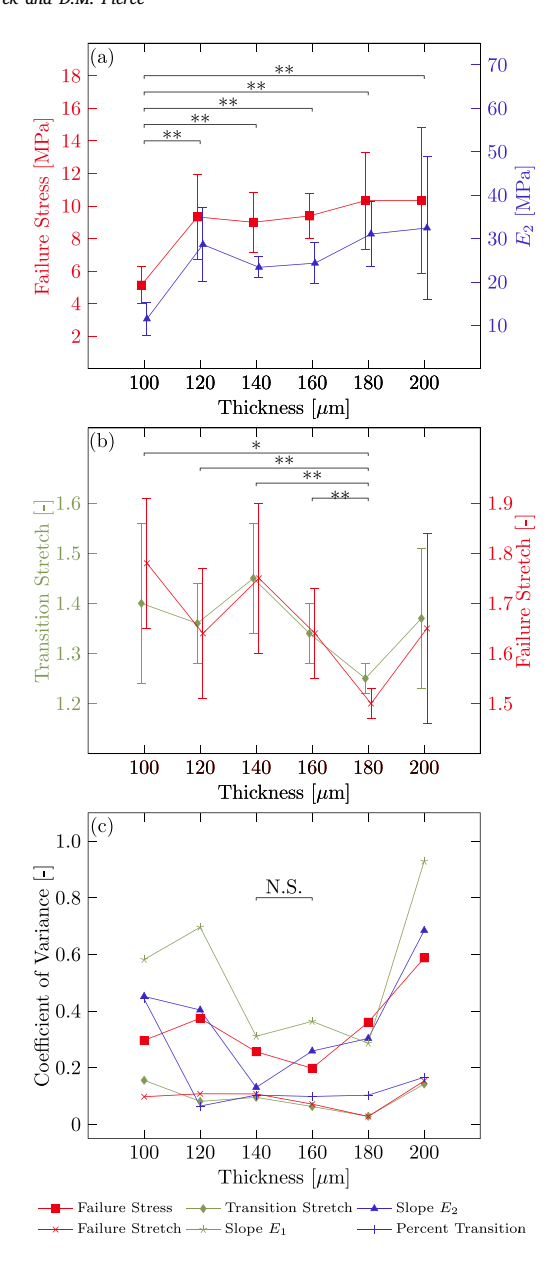


Fig. 3. Effects of specimen thickness on measured mechanical parameters: (a) Thickness of the specimen affected both the failure stress  $\sigma_f$  and final modulus  $E_2$  determined from the test with a significant difference between the 100 µm group and all other specimens (mean  $\pm$  95% confidence interval). (b) The transition stretch  $\lambda_f$  and failure stretch  $\lambda_f$  determined from the test with a significant difference between the 180 µm group and all thinner specimens (mean  $\pm$  95% confidence interval). (c) The coefficients of variance for all mechanical parameters determined from the test using the 140 µm and 160 µm thick specimens presented no significant differences while all other comparisons among thicknesses yielded at least one significant difference in variance. \* Significant differences for  $\lambda_f$ . \*\* Significant difference for both measures. N.S. No significant differences for any measures.

## 4.1. Networks of isolated collagen

Our aims in establishing a digestion protocol were to reduce time, cost, and damage to collagen while removing PG sufficient to conclude that the bulk mechanical response resulted only from the collagen network. Since we did not detect a measurable change in the inplane (2-D) reference configuration after digestion, we assumed that the corresponding change in the thickness was similarly negligible (and

most likely unmeasurable given the much smaller initial dimension). Complete removal of PG from cartilage would likely require extreme concentrations or durations that would likely damage the collagen. Thus, we targeted greater than 95% removal with a relatively inexpensive, one-step digestion protocol with the understanding that the remaining PG consists of less intricate complexes effectively eliminating its contribution to the mechanical stiffness. It remains possible that collagen was damaged during our protocol yet remained in the tissue so that we included it in the total collagen content measured after digestion. Trypsin can degrade collagen, however based on the concentration and duration we suggest, along with the quantification of collagen content post digestion, it is highly likely that we did not damage the collagen network (Chun et al., 1986). Previous researchers used trypsin in models of early osteoarthritis, intending damage to PG prior to damage to collagen, further supporting our use of trypsin to remove PG while leaving collagen intact (Griffin et al., 2014; Wang et al., 2016; Jambor et al., 2021). One of these studies specifically confirmed that the depth of penetration for effective removal of PG in cartilage by trypsin is greater than 200 µm from the articulating surface (Griffin et al., 2014). Additionally, we performed our digestion tests on 200 um-thick specimens while our final protocol recommends specimens with a thickness of 140–160 um. With a thinner specimen our digestion protocol removes more PG and likely has no further effect on collagen (i.e. no distinguishable effect).

We extracted reasonably large samples from the patellofemoral groove (to produce our tensile specimens) due to the relatively flat surface and uniform fiber orientation. While the femoral condyle or tibial plateau may better represent a load-bearing region within cartilage, the curvature of both of these surfaces make it challenging to extract flat specimens larger than a few millimeters. We considered removing "load-bearing" cartilage from the subchondral bone and flattening it before cutting with the microtome, but the additional handling and deformation would likely disturb the tissue severely. Fortunately the femoral condyle and patella present similar collagen and PG content, thus supporting our use of cartilage harvested from the patellofemoral groove for evaluation of digestion protocols (Li et al., 2021).

## 4.2. Footprint of the specimens

Our aims in determining the footprint (shape) of the specimens included homogeneity of the stress within the gauge region, manufacturability of the required specimen cutter (e.g. creating the inner radius), compatibility with displacement and force specifications of our microtensile device (§2.2), and minimizing the cartilage required for each specimen. The ASTM standard for microtensile testing was too large for the cartilage available within the bovine joint (especially if accounting for the split-line direction), so we used this standard as an initial design for our parametric finite element analyses to ensure that our revised design retained stress-strain homogeneity within the gauge region. We fixed the clamp length and width to ensure adequate surface area for gripping within the fixture. Homogeneity of the stress within the gauge region makes the subsequent stress-strain analyses straight-forward and reliable. We carefully established the footprint of our specimens to facilitate designing a specialized cutting device to efficiently prepare repeatable, uniform specimens. We ensured that specimens would fail within the force-displacement constraints of our microtensile device while minimizing the cartilage required for each specimen to ensure efficient use of each bovine joint.

# 4.3. Thickness of the specimens

Our aims in establishing the specimen thickness included remaining within the superficial zone and minimizing the thickness while avoiding potential edge effects from preparation (i.e. surface damage). If the specimen was too thin we may begin to see softening due to damage at the surface from preparation. If the specimen was too thick it may

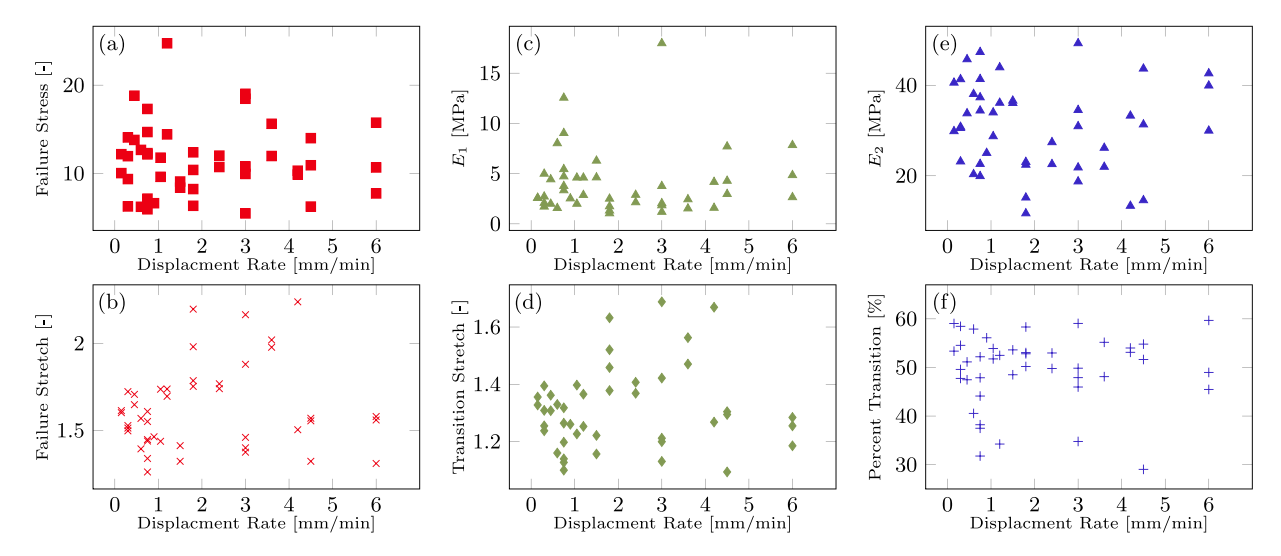


Fig. 4. Effects of Displacement rate on measured mechanical parameters: (a) failure stress, (b) failure stretch, (c) initial modulus  $E_1$ , (d) transition stretch, (e) final modulus  $E_2$ , and (f) percent transition. Within the range tested, the displacement rate had no statistically significant effects on the measured mechanical parameters.

contain both the superficial and the middle zones, thus reducing the alignment of fibers within the network (i.e. the middle zone generally presents less alignment) and convoluting subsequent interpretations of the resulting data. Our results show evidence of both extremes. We found a significant decrease in failure stress and stiffness (evident in the slope  $E_2$ ) once the specimen thickness was less than 120 µm. We also saw a significant difference in the transition and failure stretches among the specimens of 180 µm thickness and all thinner specimens. Perhaps we did not see a significant difference between the specimens of  $200 \ \mu m$ thickness and all thinner specimens due to the high variance in the 200 µm group. The particularly low variance in all of the measured mechanical parameters for the specimens of 140–160 µm thickness supports the repeatability of our proposed protocol. In practice specimens with thicknesses greater than 200 µm likely include the middle zone and specimens less than 100 µm in thickness are very difficult to handle (e.g. tearing or deforming under careful manipulation).

## 4.4. Device

We based the force and displacement requirements of our microtensile testing device on the rupture stress and strain of tensile specimens of cartilage (Kempson et al., 1973; Huang et al., 2005; Sasazaki et al., 2006).

#### 4.5. Strain rate

We aimed to determine a strain/displacement rate for tensile testing that ensured strain-rate independence while remaining time efficient. We expected to find strain-rate dependence in the mechanical parameters determined in our microtensile tests  $(\sigma_f, \lambda_f, E_1, \lambda_i, E_2, \text{ and percent transition})$  but we found no significant differences in the range of rates we explored. We concluded that strain rates between 1.5 and 60%/min (displacement rates between 150 and 6000  $\mu\text{m/min})$  produce mechanical results independent of strain rate. Strain rates below this range only increase the total time required for mechanical testing. Strain rates higher than this introduced significant noise into the mechanical data, noise resulting from the rapid motion of the actuator.

Considering the viscous effects we should expect from collagen fibers alone within our proposed range of strain rates (1.5–60%/min), our findings agree with the current literature. Time constants related to mechanical relaxation (viscous effects) of collagen are on the order of 100 s (Ahsanizadeh and Li, 2015; Pierce et al., 2016), while all of the tests here were longer (average test length  $\sim$ 20 min). The upper extreme of our proposed range of strain rates (equivalent to

1%/sec) is also below that considered a quasi-static strain-rate for visco-hyperelastic modeling of tendon and cartilage (Ahsanizadeh and Li, 2015).

#### 4.6. Limitations and outlook

There are limitations to our proposed specimen dimensions. We assumed specimens were homogeneous through the thickness based on proportional definitions of through-thickness zones (Mow et al., 2005). We thus assumed that each specimen represented only the superficial zone and that each was unaffected by the fiber orientation inherent to the middle zone. We did not evaluate the principal fiber orientation within each individual specimen. Additional, we removed the top-most superficial zone (10-20 µm of the articular surface) to remove other fibrillar collagens (i.e. types I and III) along with functional proteins involved in joint mobility (Ghadially et al., 1982; Fujioka et al., 2013; Flowers et al., 2017). This method of preparation limits the number of specimens per knee to ~24 (best case). We assumed incompressibility in calculating the Cauchy stresses from our measured data. Finally, we chose to use grip-to-grip stretch in our mechanical analyses which introduced approximately 1-6% error in the stretch. To reduce this error, future users may measure strain in the gauge region using optical methods or use the grip-to-grip strain adjusted by the approximate error, cf. Appendix A.

Mechanical testing of isolated networks of type II collagen fibers leveraging this protocol will lead to better understanding of the mechanics both of these networks and of the individual collagen fibers. Such understanding may aid in the development and testing of therapeutics aimed at repairing damaged tissues, e.g. those developed to treat diseases of articular cartilage which present changes in fiber organization and bulk softening such as osteoarthritis (Matzat et al., 2013; Szarek et al., 2020). Isolating collagen networks from osmoticallyinduced pretension may also aid in understanding inter-constituent interactions and their roles in bulk tissue biomechanics. Our protocol may aid researchers in investigating the effects of mechanical loading (e.g. repeated, damage-inducing, rate-dependence) and biochemical modifications (e.g. temperature, +/-crosslinking, cell products) on networks of type II collagen, an essential mechanical constituent within tissues and engineered biomaterials. Such data and understanding may also be leveraged to propose, calibrate, and validate constitutive and multiscale models for finite element analyses of soft tissues. Finally, our protocol could also be adapted to study other collagen-rich tissues and biomaterials.

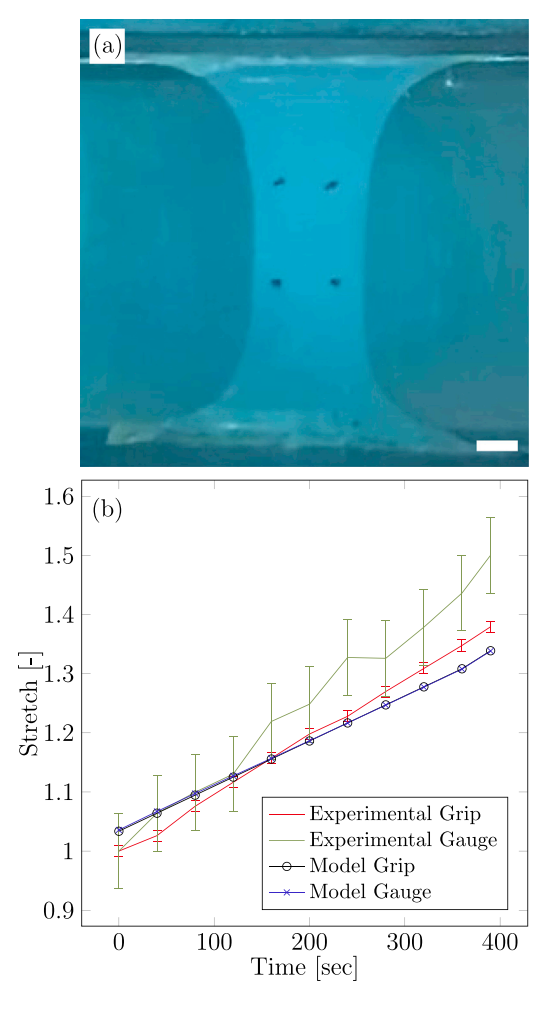
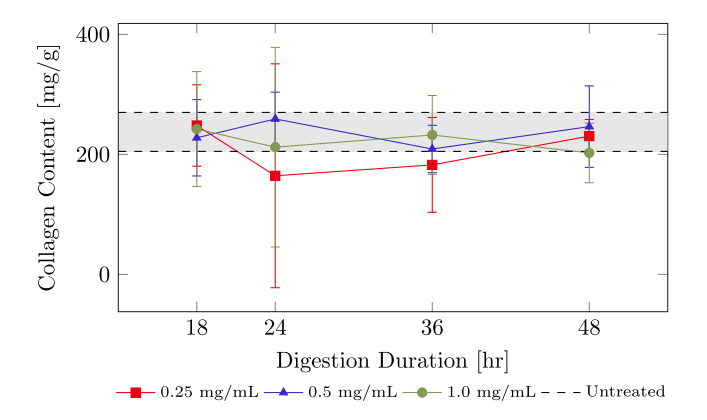
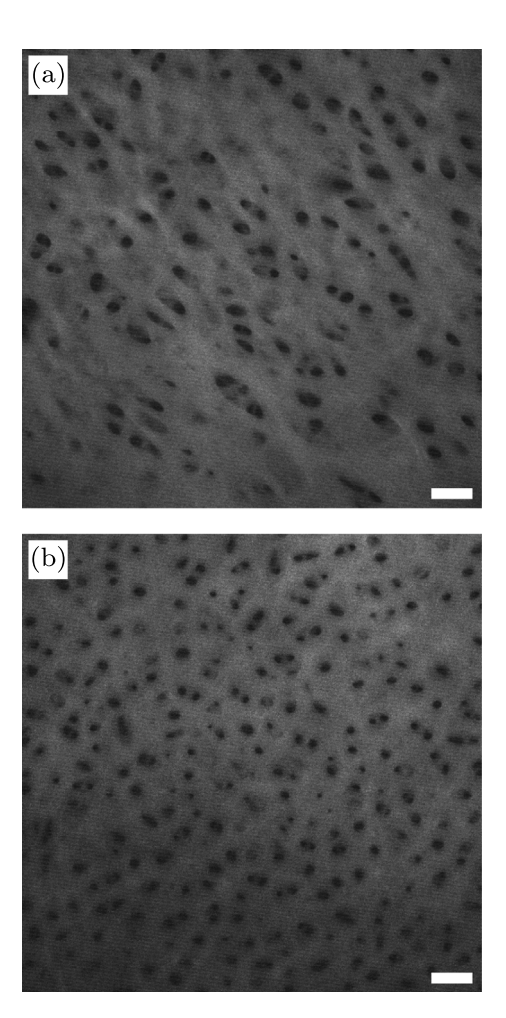


Fig. 5. Experimental and computations studies using the specimen geometry reveal that stretches estimated from grip-to-grip measurements provide good approximations to those estimated from measurements in the gauge region. (a) We estimated stretches experimentally using measurements of both the grip-to-grip distance and the distance between markers within the gauge region using images with a resolution of 0.09 mm. Bar = 1 mm. (b) We estimated stretches computationally using measurements of the grip-to-grip distance within our finite element analyses and using the deformation gradient extracted from elements within the gauge region of the same model. Use of the grip-to-grip stretch in our mechanical analyses introduced approximately  $1\%{-}6\%$  error in the stretch.



**Fig. 6.** Collagen content after trypsin digestion. All digestion protocols that removed >95% of the proteoglycan from cartilage were not significantly different from each other nor from health untreated specimens in regard to the final collagen content (Maier et al., 2019a). Median and interquartile range shown for each digestion protocol and for untreated specimens serving as controls.



**Fig. 7.** Our digestion protocols induced mild microstructural changes in the collagen network of cartilage. Second harmonic generation (SHG) images: (a) native and (b) trypsin-digested specimens of cartilage. Bar =  $200~\mu m$ .

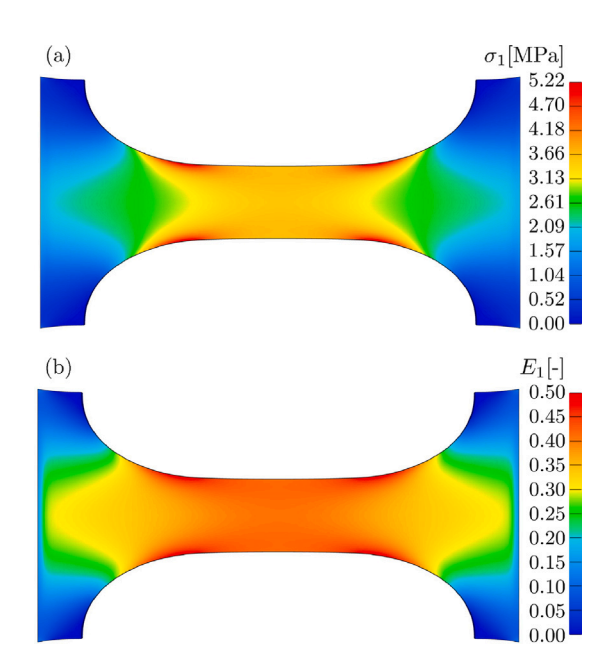


**Fig. 8.** Finite element analyses of the proposed testing specimen at applied stretch = 1.3. (a) First principal stresses (MPa) and (b) first principal Lagrangian strains are nearly uniform at the center of the gauge region.

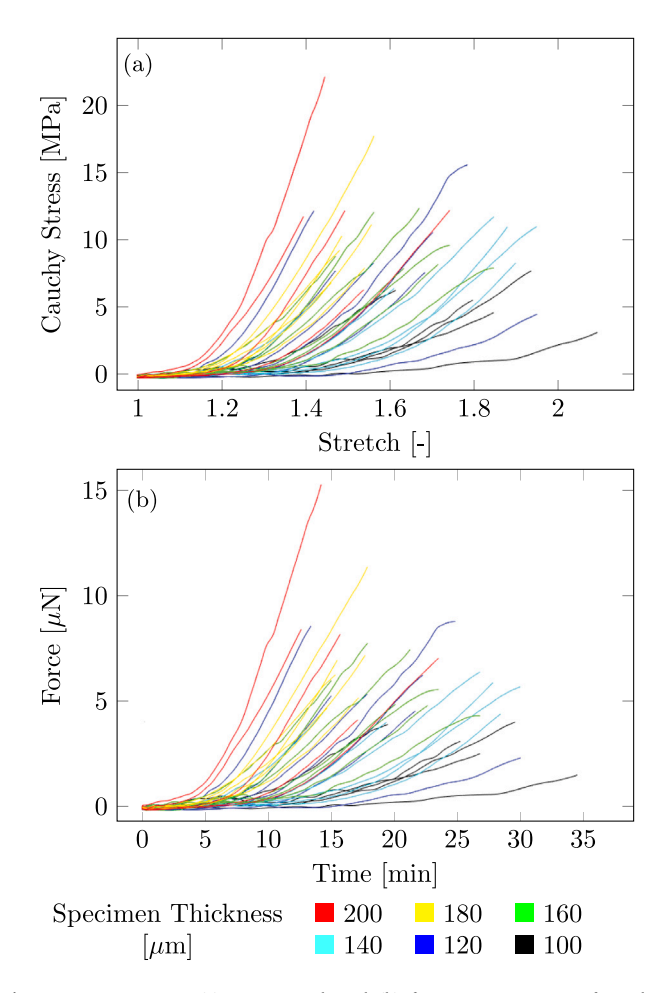


Fig. 9. Representative (a) stress–stretch and (b) force–time responses of cartilage specimens with thicknesses ranging from 100 to 200  $\mu m$ .

## Role of the funding source

The National Science Foundation and the GAANN Fellowship had no involvement in the study design; in collection, analysis and interpretation of data; in the writing of the manuscript; or in the decision to submit the manuscript for publication. Any opinions, findings, and conclusions or recommendations expressed in this material are those of the author(s) and do not necessarily reflect the views of the National Science Foundation.

## CRediT authorship contribution statement

**Phoebe Szarek:** Conception and design, Prepared specimens, Conducted experiments, Analyzed and interpreted data, Writing – original draft, Writing – review & editing. **David M. Pierce:** Oversaw the project, Conception and design, Analyzed and interpreted data, Writing – original draft, Writing – review & editing.

## Declaration of competing interest

The authors declare the following financial interests/personal relationships which may be considered as potential competing interests: David M. Pierce reports financial support was provided by National Science Foundation. Phoebe Szarek reports financial support was provided by GAANN.

#### Data availability

Data will be made available on request.

#### Acknowledgments

We thank the National Science Foundation CAREER 1653358, the U.S. Department of Education GAANN P200A160323, and the UConn GE Fellowship for funding. We also thank UConn Statistics Consulting Services, and Christopher Lemay, Zachary Ohayon, and Anthony Rivera. All authors approved the version of the manuscript to be published.

#### Appendix A

Experimental and computational estimates of stretches calculated from grip-to-grip versus gauge-region measurements reveal minimal error in the method using grip-to-grip measurements, see Fig. 5.

#### Appendix B

All digestion protocols we tested did not remove a significant amount of collagen from cartilage, see Fig. 6.

However, our digestion protocol induced mild microstructural changes in collagen structure, see Fig. 7.

#### Appendix C

Finite element analyses of the footprint of the proposed testing specimen revealed that the gauge region experiences relatively constant first principal stresses and strains, see Fig. 8.

## Appendix D

Representative mechanical responses of the cartilage specimens with thicknesses ranging from 100 to 200  $\mu$ m, see Fig. 9.

# Appendix E. Mechanical testing of type II collagen networks

We propose the following protocol for tensile testing of type II collagen networks isolated from cartilage.

## Specimen extraction

- 1. Source bovine knee joints (also known as stifle joints) from animals less than 36 months of age.
- 2. Remove soft tissues (excluding cartilage) and expose the articular surfaces within the joint.
  - Maintain tissue hydration with phosphate-buffered saline (PBS) either by spraying the joint surface or submerging in bath of PBS.
- 3. Secure the femur with the patellofemoral groove facing up (e.g. with a bench vise).
- Extract 10 mm by 20 mm full-thickness cuboid specimen of cartilage including some subchondral bone using a #18 blade and hammer.
  - Ensure that the long edge is perpendicular to the length of the patellofemoral groove and do not fracture the bone as this may deform or wrinkle the cartilage.
  - Place the extracted cuboids in bath of PBS.

#### Specimen slicing and preparation

- Add 2.722 g of disodium phosphate (Na<sub>2</sub>HPO<sub>4</sub>) and 3.506 g of sodium chloride (NaCl) to 400 mL of distilled water to use as buffer moving forward. Make fresh buffer as needed.
- 2. Mount the cartilage–bone cuboid specimen by clamping the bone into the sample holder of a microtome.
- Keep the surface of the tissue hydrated by using a pipette to drip buffer onto the surface.
- 4. Adjust the microtome speed so the cut occurs quickly enough that the blade slices the tissue (instead of pressing out the fluid within the tissue). Adjust the slice thickness to 20 μm.
- 5. Slowly advance the microtome until it makes contact with the tissue and slices the most superficial surface (10–20  $\mu$ m). Stop the microtome.
- 6. Adjust the slice thickness to between 140 and 160  $\mu m$ .
- 7. Slice one layer and handle sliced specimens with care using forceps or a paint brush. Only handle the specimen on the edges to avoid damaging the specimen within what will become the dumbbell shape.
- Place slice on a flat cutting surface and use the specimen punch to cut the dumbbell-shaped specimen. Place punched specimens in bath of buffer.

#### Enzymatic digestion

- Store trypsin at a concentration of 50mg/mL in 1 mL aliquots at -20 °C. (Dilute to 0.5 mg/mL, by adding 1 mL of stock solution with 49 mL of buffer.)
- 2. Mix 0.5 mg/mL trypsin in buffer solution.
- 3. Add specimens to solution within a heat-resistant, sealed container (e.g. 50 mL centrifuge tubes work well).
- 4. Incubate specimens for 18 h at 37 °C.
- Rinse specimens on a rocker table three times in buffer for 5 minutes each time.

#### Mechanical testing

- 1. Clamp the ends of each specimen using sandpaper and cyanoacrylate glue. Place a weight on each end and a drop of buffer on the gauge region while the glue is drying (~3 min).
- 2. Mount specimen in the microtensile device in a bath of buffer at  $25\,^{\circ}C$
- Apply a tensile displacement until the force reads 0.01 N. Slightly relax the displacement.
- 4. Equilibrate for 300 s.
- 5. Run tensile test to failure at a displacement rate between 150 and  $6000~\mu\text{m/min}$ .

#### References

- Ahsanizadeh, S., Li, L., 2015. Visco-hyperelastic constitutive modeling of soft tissues based on short and long-term internal variables. Biomed. Eng. Online 14, 29.
- American Society for Testing Materials, 2013. Standard test method for tensile properties of plastics by use of microtensile specimens. Tech. Rep., (D1708-13), American Society for Testing Materials, 100 Barr Harbor Drive, PO Box C700, West Conshohocken, PA.
- Andriacchi, T.P., Mündermann, A., 2006. The role of ambulatory mechanics in the initiation and progression of knee osteoarthritis. Curr. Opin. Rheumatol. 18, 514–518
- Aspden, R., 1994. Fibre reinforcing by collagen in cartilage and soft connective tissues. Proc. R. Soc. Lond. B 258, 195–200.
- Below, S., Arnoczky, S.P., Dodds, J., Kooima, C., Walter, N., 2002. The split-line pattern of the distal femur: A consideration in the orientation of autologous cartilage grafts. Arthroscopy 18, 613–617.
- Broom, N.D., Marra, D.L., 1986. Ultrastructural evidence for fibril-to-fibril associations in articular cartilage and their functional implication. J. Anat. 146, 185–200.
- Bustamante, C., Bryant, Z., Smith, S., 2003. Ten years of tension: single-molecule DNA mechanics. Nature 421, 423–427.

- Cai, H., Hao, Z., Xiao, L., Wan, C., Tong, L., 2017. The collagen microstructural changes of rat menisci and tibiofemoral cartilages under the influence of mechanical loading: An in vitro wear test of whole joints. 25, S207–S217.
- Chun, L., Koob, T., Eyre, D., 1986. Sequential enzymatic dissection of the proteoglycan complex from articular cartilage [abstract]. Trans. Orthop. Res. Soc. 11, 96.
- Elliot, D., Guilak, F., Vail, T., Wang, J., Setton, L., 1999. Tensile properties of articular cartilage are altered by meniscectomy in a canine model of osteoarthritis. J. Orthop. Res. 17, 503–508.
- Eppell, S., Smith, B., Kahn, H., Ballarini, R., 2006. Nano measurements with microdevices: mechanical properties of hydrated collagen fibrils. J. R. Soc. Interface 3, 117–121.
- Flowers, S., Zieba, A., Örnros, J., Jin, C., Rolfson, O., Björkman, L., Eisler, T., Kalamajski, S., Kamali-Moghaddam, M., Karlsson, N., 2017. Lubricin binds cartilage proteins, cartilage oligomeric matrix protein, fibronectin and collagen II at the cartilage surface. Sci. Rep. 7, 13149.
- Fujioka, R., Aoyama, T., Takakuwa, T., 2013. The layered structure of the articular surface. Osteoarthr. Cartil. 21, 1092–1098.
- Gestos, A., Whitten, P., Spinks, G., Wallace, G., 2013. Tensile testing of individual glassy, rubbery and hydrogel electrospun polymer nanofibres to high strain using the atomic force microscope. Polym. Test. 32, 655–664.
- Ghadially, F., Yong, N., Lalonde, J.-M., 1982. A transmission electron microscopic comparison of the articular surface of cartilage processed attached to bone and detached from bone. J. Anat. 135, 685–706.
- Goss, C., Croquette, V., 2002. Magnetic tweezers: Micromanipulation and force measurement at the molecular level. Biophys. J. 82, 3314–3329.
- Gottardi, R., Hansen, U., Raiteri, R., Loparic, M., Düggelin, M., Mathys, D., Friederich, N.F., Bruckner, P., Stolz, M., 2016. Supramolecular organization of collagen fibrils in healthy and osteoarthritic human knee and hip joint cartilage. PLoS One 11, e0163552.
- Griffin, D.J., Vicari, J., Buckley, M.R., Silverberg, J.L., Cohen, I., Bonassar, L.J., 2014. Effects of enzymatic treatments on the depth-dependent viscoelastic shear properties of articular cartilage. J. Orthop. Res. 32, 1652–1657.
- Huang, C., Stankiewicz, A., Ateshian, G.A., Mow, V., 2005. Anisotropy, inhomogeneity, and tension-compression nonlinearity of human glenohumeral cartilage in finite deformation. J. Biomech. 38, 799–809.
- Hukins, D., Leahy, J., Mathias, K., 1999. Biomaterials: defining the mechanical properties of natural tissues and selection of replacement materials. J. Mater. Chem. 9, 629–636.
- Jambor, A.N., Shelton, E.M., Kijowski, R., Henak, C.R., Campagnola, P.J., 2021.
  Assessing collagen alterations in enzymatic degradation models of osteoarthritis via second harmonic generation microscopy. Osteoarthr. Cartil. 29, 1590–1599.
- Kadler, K., Hill, A., Canty-Laird, E., 2008. Collagen fibrillogenesis: fibronectin, integrins, and minor collagens as organizers and nucleators. Curr. Opin. Cell Biol. 20, 495–501
- Karvonen, R., Fernandez-Madrid, F., Lande, M., Hazlett, L., Barrett, R., An, T., Huebner, C., 1991. Proteoglycans from osteoarthritic human articular cartilage influence type II collagen in vitro fibrillogenesis. Connect. Tissue Res. 27, 235–250.
- Kempson, G.E., Muir, H., Pollard, C., Tuke, M., 1973. The tensile properties of the cartilage of human femoral condyles related to the content of collagen and glycosaminoglycans. Biochim. Biophys. Acta 297, 456–472.
- Kempson, G.E., Muir, H., Swanson, S.A.V., Freeman, M.A.R., 1970. Correlations between stiffness and the chemical constituents of cartilage on the human femoral head. Biochim. Biophys. Acta 215, 70–77.
- Kuijer, R., van de Stadt, R., de Koning, M., van der Korst, J., 1985. Influence of constituents of proteoglycans on type II collagen fibrillogenesis. Coll. Relat. Res 5, 379–391.
- Lee, S., Piez, K., 1983. Type II collagen from lathyritic rate chondrosarcoma: preparation and *in vitro* fibril formation. Coll. Relat. Res. 3, 89–103.
- Li, H., Li, J., Yu, S., Wu, C., Zhang, W., 2021. The mechanical properties of tibiofemoral and patellofemoral articular cartilage in compression depend on anatomical region. Sci. Rep. 11, 6128.
- Liu, Y., Ballarini, R., Eppell, S., 2016. Tension tests on mammalian collagen fibrils.
- Maas, S.A., Ellis, B.J., Ateshian, G.A., Weiss, J.A., 2012. FEBio: finite elements for biomechanics. J. Biomech. Eng. 134, 011005.
- Maier, F., Lewis, C.G., Pierce, D.M., 2019a. The evolving large-strain shear responses of progressively osteoarthritic human cartilage. Osteoarthr. Cartil. 27, 810–822.
- Maier, F., Lewis, C.G., Pierce, D.M., 2019b. Through-thickness patterns of shear strain evolve in early osteoarthritis. Osteoarthr. Cartil. 27, 1382–1391.
- Matzat, S., van Tiel, J., Gold, G., Oei, E., 2013. Quantitative MRI techniques of cartilage composition. Quant. Imaging Med. Surg. 3, 162–174.
- McNulty, M., Mahmud, A., Spiers, P., Feely, J., 2006. Collagen type-i degredation is related to arterial stiffness in hypertensive and normotensive subjects. J. Hum. Hypertens. 20, 867–873.
- Miyazaki, H., Hayashi, K., 1999. Tensile tests of collagen fibers obtained from the rabbit patellar tendon. Biomed. Microdev. 2, 151–157.
- Mow, V.C., Gu, W.Y., Chen, F.H., 2005. Structure and function of articular cartilage and meniscus. In: Mow, V.C., Huiskes, R. (Eds.), Basic Orthopaedic Biomechanics & Mechano-Biology, third ed. Lippincott Williams & Wilkins, Philadelphia, pp. 181–258.

- Onur, T., Wu, R., Metz, L., Dang, A., 2014. Characterisation of osteoarthritis in a small animal model of type 2 diabetes mellitus. Bone Joint Res. 3, 203–211.
- Ottani, V., Raspanti, M., Ruggeri, A., 2001. Collagen structure and functional implications. Micron 32, 251–260.
- Park, S., Hung, C., Ateshian, G., 2004. Mechanical response of bovine articular cartilage under dynamic unconfined compression loading at physiological stress levels. Osteoarthr. Cartil. 12, 65–73.
- Pierce, D.M., Unterberger, M.J., Trobin, W., Ricken, T., Holzapfel, G.A., 2016. A microstructurally based continuum model of cartilage viscoelasticity and permeability incorporating statistical fiber orientation. Biomech. Model. Mechanobiol. 15, 229–244.
- Quigley, A., Bancelin, S., Deska-Gauthier, D., Légaré, F., Veres, S., Kreplak, L., 2018.
  Combining tensile testing and structural analysis at the single collagen fibril level.
  Sci. Data 5.
- Ricard-Blum, S., 2011. The collagen family. Cold Spring Harb. Perspect. Biol. 3, a004978.
- Sasazaki, Y., Shore, R., Seedhom, B.B., 2006. Deformation and failure of cartilage in the tensile mode. J. Anat. 208, 681–694.
- Stender, C., Rust, E., Martin, P., Neumann, E., Brown, R., Lujan, T., 2018. Modeling the effect of collagen fibril alignment on ligament mechanical behavior. Biomech. Model. Mechanobiol. 17, 543–557.
- Szarek, P., Lilledahl, M., Emery, N., Lewis, C., Pierce, D., 2020. The zonal evolution of collagen-network morphology quantified in early osteoarthritic grades of human cartilage. Osteoarthr. Cartil. Open 2, 100086.
- Szarko, M., Muldrew, K., Bertram, J.E.A., 2010. Freeze-thaw treatment effecs on the dynamic mechanical properties of articular cartilage. BMC 566 Musculoskelet. Disord 11

- Taye, N., Karoulis, S.Z., Hubmacher, D., 2019. The "other" 15-40%: The role of non-collagenous extracellular matrix proteins and minor collagens in tendon. J. Orthop. Res. 38, 23–35.
- Torzilli, P., Arduino, J., Gregory, J., Bansal, M., 1997. Effect of proteoglycan removal on solute mobility in articular cartilage. J. Biomech. 30, 895–902.
- van der Rijt, J., van der Werf, K., Bennink, M., Dijkstra, P., Feijen, J., 2006.

  Micromechanical testing of individual collagen fibrils. Macromol. Biosci. 6, 697–702
- Wale, M., Nesbitt, D., Henderson, B., Fitzpatrick, C., Creechley, J., Lujan, T., 2021.
  Applying ASTM standards to tensile tests of musculoskeletal soft tissue: Methods to reduce grip failure and promote reproducibility. J. Biomech. Eng. 143, 011011.
- Wan, J., Zhang, G., Li, X., Qui, X., Ouyang, J., Dai, J., Min, S., 2021. Matrix metalloproteinase 3: A promoting and destabilizing factor in the pathogenesis of disease and cell differentiation. Front. Physio. 12, 663978.
- Wang, X., Eriksson, T., Ricken, T., Pierce, D., 2018. On incorporating osmotic prestretch/prestress in image-driven finite element simulations of cartilage. J. Mech. Beh. Biomed. Mat. 86. 409–422.
- Wang, K., Wu, J., Day, R., Kirk, T., Hu, X., 2016. Characterizing depth-dependent refractive index of articular cartilage subjected to mechanical wear or enzymic degeneration. J. Biomed. Opt. 21, 095022.
- Wenger, M., Bozec, L., Horton, M., Mesquida, P., 2007. Mechanical properties of collagen fibrils. Biophys. J. 93, 1255–1263.
- Williamson, A.K., Chen, A.C., Masuda, K., Thonar, E.J., Sah, R.L., 2003. Tensile mechanical properties of bovine articular cartilage: Variations with growth and relationships to collagen network components. J. Orthop. Res. 21, 872–880.
- Zhu, W.B., Mow, V.C., Koob, T.J., Eyre, D.R., 1993. Viscoelastic shear properties of articular cartilage and the effects of glycosidase treatments. J. Orthop. Res. 11, 771-781.